IEEE Access
Multidisciplinary | Rapid Review | Open Access Journal

Received March 15, 2022, accepted April 1, 2022, date of publication April 5, 2022, date of current version April 28, 2022.

Digital Object Identifier 10.1109/ACCESS.2022.3165091

Finite-Time Fault-Tolerant Control for a Stewart Platform Using Sliding Mode Control With Improved Reaching Law

DUC-VINH LE AND CHEOLKEUN HA
Department of Mechanical Engineering, University of Ulsan, Ulsan 44610, South Korea
Corresponding author: Cheolkeun Ha (cheolkeun@gmail.com)

ABSTRACT In this paper, a fault-tolerant control (FTC) is proposed for a nonlinear system as a Stewart platform (SP). To reject the singularity issue of a traditional fast terminal sliding mode control (FTSMC) and to have a fast finite-time convergence, a nonsingular fast terminal sliding mode control (NFTSMC) is used. In addition, an extended state observer (ESO) is applied for the control scheme to estimate uncertainties, disturbances, and faults. To increase the convergence speed and alleviate the chattering phenomenon, a novel reaching law is proposed which gives the system a quick reaching speed. Finally, a novel FTC that ensures robustness to disturbances and faults is developed based on the NFTSMC, the ESO, and the proposed reaching law. Consequently, the proposed FTC has outstanding features such as high tracking performance, a decrease in the effects of disturbances and faults, a fast convergence speed in finite time, and less chattering. The simulation and experiment results demonstrate the efficiency of the proposed FTC compared to other control schemes.

INDEX TERMS Fault tolerant control, sliding mode control, reaching law, extended state observer, Stewart platform.

I. INTRODUCTION

Robots play an increasingly important role in human life these days. They are used to perform complicated tasks in many fields such as industrial manufacturing, medicine, civil engineering, and aerospace. Nevertheless, in practice, we have to face some inevitable problems during the operation of robots, such as uncertainty, disturbances, and unmodeled dynamics and friction which may lead to a serious destabilization of the system. This has caused great obstacles and challenges in designing controllers for robot manipulators. Therefore, the requirement for precise and robust control has attracted a massive number of researchers over the past decades. Various solutions to improving robot performance have been developed, such as adaptive control [1], [2], neural network control [3], [4], and sliding mode control (SMC) [5]–[7] for nonlinear systems in general and for the Stewart platform (SP) in particular.

A SP is a parallel manipulator that has six prismatic actuators connecting the fixed base and the moving platform. Thanks to its outstanding benefits of high precision, good rigidity, and higher payloads compared with other serial robots, it is extensively applied in industry, telescopes, flight and vehicle simulators, entertainment, and medical instruments [8]–[10]. Nonetheless, due to the inherent complexity in the kinetic analysis of its closed-loop structure, the application of a SP is often challenging. Hence, various kinematic and dynamic investigations have been reported in the literature [11]–[14], and several control technologies for the SP have been studied over the years [2], [4], [7]. Among them, SMC possesses fascinating characteristics of robustness to disturbances and uncertainties, and low sensitivity to noise. Nevertheless, conventional SMC cannot ensure that the states of the system approach the equilibrium point in finite time.

Therefore, to ensure that the system state quickly converges in finite time, Nonsingular Fast Terminal Sliding mode control (NFTSMC) was developed and has received much attention from many researchers [5], [6]. It not only preserves the robustness of the traditional SMC, but also has fast convergence in finite time and avoids the singularity issue of Fast Terminal Sliding mode control (FTSMC). Although NFTSMC has many advantages, in practice there might be

The associate editor coordinating the review of this manuscript and approving it for publication was Jesus Felez.

faults occurring in the system and NFTSMC alone cannot ensure the stability of the system. Therefore, there have been many investigations of this problem over the years, and some fault-tolerant technologies have been proposed to increase the safety of robotic systems.

In general, there are two major types of Fault-tolerant control (FTC): passive FTC (PFTC) [15], [16] and active FTC (AFTC) [17], [18]. A PFTC is designed without a fault diagnosis module for normal and fault operation, and depends on the robust capability of the controllers to address lumped disturbances, uncertainty, and faults. The most notable feature of PFTC is its quick response to the occurrence of faults because it does not take time to wait for the fault feedback; however, its ability to compensate for high-magnitude faults is restricted. As a result, there are some limitations in the application of PFTC in actual systems.

In contrast, the key feature of AFTC is its use of an estimation module to compensate for the unpredictable faults in mechanical components, sensors, and actuators to preserve the stability of the system within performance requirements. The robust response of AFTC to faults primarily depends on the efficiency of the estimation module. Hence, a series of active fault-tolerant strategies have been developed for robotic systems based on various observers, such as the sliding mode observer [19], the fuzzy observer [17], and the extended state observer (ESO) [18]. Compared to the other methods, the ESO is an efficient way to estimate faults and is easy to implement in practice. Nonetheless, it is well known that the conventional ESO has several drawbacks, such as the peaking phenomenon that can cause serious stability deterioration of the overall system [20], and its trade-off between the speed of estimation and insensitivity to measurement noise [21]. Many researchers have introduced solutions to decreasing the magnitude of peaking and ensuring the robustness to measurement noise [22]–[24]. In [24], Ran *et al.* proposed a new ESO that was effective in lessening the peaking issue and had improved sensitivity to measurement noise. Thus, given the significant benefits mentioned above, in this study a NFTSMC and an ESO [24] are applied in a FTC scheme to considerably improve its performance regardless of the presence of faults in the SP.

Although the accuracy of the system can be improved by the FTC schemes described above, researchers have developed various methods to speed up the reaching rate and diminish chattering which is a major issue in SMC. The chattering problem not only destabilizes the system but also seriously affects its practical applications. Hence, it is of great interest to resolve this issue, and strategies such as the boundary layer method [25], [26], high-order SMC [27], [28], and the reaching law SMC method [29]–[33] have been developed. Of these, the reaching law SMC has attractive advantages due to not only its ability to effectively decrease the chattering issue, but also to improve the approaching phase rate.

In [29], three continuous-time reaching laws were proposed by Gao and Hung First, the constant rate reaching law is a simple method that makes the state slide on the sliding surface at a constant rate. Its drawback is the trade-off between the speed of the approaching phase and the magnitude of oscillation in the sliding phase. Next, a modification to the constant reaching law, called the constant plus proportional rate reaching law, can reduce the oscillation to a certain level. The final method is the power rate reaching law, which can decrease chattering.

Based on these methods, several other deep investigations on reaching law have been produced over the years. Wang *et al.* [30] used a double-power reaching law to further enhance the efficiency of the power reaching law and decline the chattering issue, and an improved double-power reaching law was proposed by Tao *et al.*[31]. Fallaha *et al.* [32] introduced the exponential reaching law, which can increase the convergence speed and reduce oscillation. Yang and Chen [33] designed a piecewise fast multi-power reaching law based on the fast-power and double-power reaching laws. Generally, the power reaching law has excellent reaching performance and less chattering.

Inspired by these aforementioned works, a new reaching law (NRL) is proposed in this paper to further reduce the reaching time and the chattering problem. The finite-time stability of this new reaching law is demonstrated, as well as its ability to give the system a fast reaching speed. The dynamic coefficient is used to accelerate the convergence rate and minimize the chattering amplitude when the system approaches the sliding surface. As a result, this paper will illustrate the performance of the proposed FTC scheme by combining NFTMSC, ESO [24], and the NRL, which has the benefits of easy implementation, singularity avoidance, robustness in uncertainties and faults, a decrease in the peaking issue, high accuracy, chattering alleviation, and rapid convergence in finite time. In the simulation and experiment parts, a comparison between the proposed FTC and the control scheme without the estimation module is shown to demonstrate the usefulness of the ESO [24] in the proposed FTC under the occurrence of faults. In addition, this paper compares the performance of the proposed FTC with the control schemes using the other reaching laws to prove the effect of the NRL on enhancing the reaching speed. Accordingly, the validity of the proposed FTC using the new ESO [24] and the proposed reaching law is evaluated.

The remainder of this study is organized as follows: The NRL is described in Section II; Section III shows the SP dynamic; the traditional ESO [34] and the new ESO [24] are introduced in Section IV; Section V illustrates the proposed FTC based on NFTSMC, the ESO [24], and the NRL. The results of the control performance in the simulation and experiment are given in Sections VI and VII, respectively. Finally, the conclusions are discussed in Section VIII.

II. A NEW REACHING LAW

As mentioned above, many valid methods have been investigated to reduce chattering in SMC. Among them, the improvement of the reaching law in SMC cannot only

eliminate the oscillation but can also approach the sliding surface rapidly. Thus, many reaching laws have been proposed, such as the quick-power reaching law (QPRL) and the double-power reaching law (DPRL), which have excellent reaching performance. The QPRL is derived by a combination of the power rate reaching and the proportional rate term with the constant coefficients and can be designed as:

$$\dot{s} = -k_1 |s|^{w_1} \operatorname{sgn}(s) - k_2 s \tag{1}$$

whereas the DPRL has two power terms and can be described as:

$$\dot{s} = -k_1 |s|^{w_1} \operatorname{sgn}(s) - k_2 |s|^{w_2} \operatorname{sgn}(s) \tag{2}$$

where $k_1 > 0, k_2 > 0, 0 < w_1 < 1, w_2 > 1$. The first part in the right hand of the DPRL (2) plays the main role when $|s| < 1$ and while the second part plays the main role when $|s| > 1$.

It is well known that the reaching speed of the QPRL (1) is slower than that of the DPRL (2) when the states of the system are far away from the sliding surface, i.e., $|s| \geq 1$, but the reaching speed of the QPRL (1) is faster than that of the DPRL (2) when the states approach the sliding surface, i.e., $|s| < 1$. Taking advantage of the benefits of the QPRL and the DPRL, a NRL is described as:

$$\dot{s} = -k_3 \tanh\left(\frac{s}{\eta}\right) - k_2 |s|^g \operatorname{sgn}(s) \tag{3}$$

where

$$k_3 = \frac{2k_1}{\varepsilon + (1-\varepsilon)\exp(-c(|s|-1))}$$

$$g = \begin{cases} r & if \ \ |s| \geq 1 \\ 1 & if \ \ |s| < 1, \end{cases} \quad r > 1, \ \text{positive constant}$$

$k_1, k_2, \varepsilon, c, \eta$ are positive constants, and $0 < \varepsilon < 1$.

In the NRL, the first coefficient and the second power terms can be dynamically changed according to the magnitude of s. In particular, the hyperbolic tangent function is used in the NRL instead of the sign function to further reduce the chattering when the system is close to the sliding surface. Figure 1 shows the value of the sign function sign(s) and tangent function tanh(s). It can be seen that the value of tanh(s) smoothly changes, and when s approaches zero, the magnitude of tanh(s) decreases dramatically to make the first term in (3) decline. It is very helpful to reject the oscillation when the system is near the sliding surface.

For example, the parameters in (1), (2), and (3) are given as $k_1 = 3$, $k_2 = 4$, $w_1 = 0.8$, $w_2 = 1.5$, $r = 1.5$, $\varepsilon = 0.1$, $\eta = 0.1$, $c = 0.2$. We test the convergence speeds of the thee reaching laws for two cases in which the initial value of s is given as $s(0) = 10$ and $s(0) = 1$. Figure 2 shows the results of the simulation for the reaching laws. As we can see, when $|s| \geq 1$, the convergence rate of the NRL (3) is faster than that of the DPRL (2). On the other hand, when $|s| < 1$, the convergence speed of (3) is faster than that of the QPRL (1).

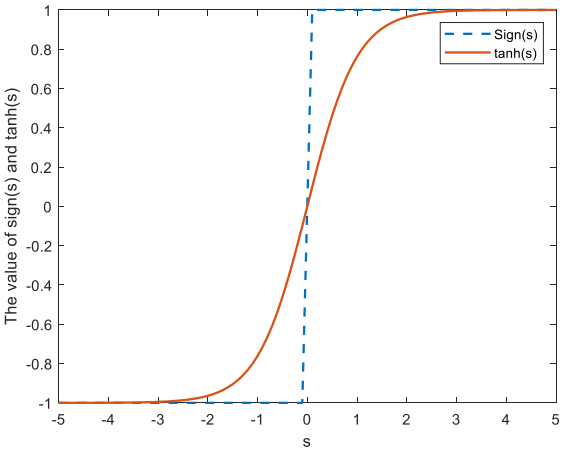

FIGURE 1. The value of function sign(s) and tanh(s).

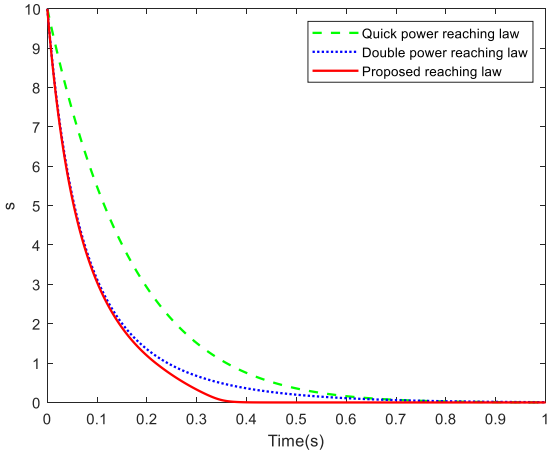

a)

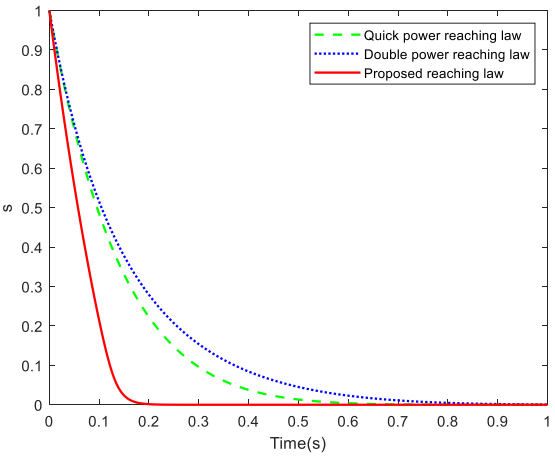

b)

FIGURE 2. The value of s. a) $s(0) = 10$; b) $s(0) = 1$.

Remark: When s approaches zero, (3) can be approximately equivalent to the following expression:

$$\dot{s} = -\frac{2k_1}{\varepsilon + (1-\varepsilon)\exp(c)} \tanh\left(\frac{s}{\eta}\right) - k_2 s \tag{4}$$

then

$$\frac{2k_1}{\varepsilon + (1-\varepsilon)\exp(c)} < \frac{2k_1}{\varepsilon + (1-\varepsilon)\exp\left(-c(|s|-1)\right)}$$

which can obtain the goal of less chattering. Therefore, the NRL cannot only have a fast reaching rate in different stages but can also decrease the chattering issue.

Convergence Analysis: For the NRL (3), selecting the Lyapunov function $V_1 = 0.5s^2$ and its derivative is:

$$\dot{V}_1 = s\dot{s} = \left(-k_3 s \tanh\left(\frac{s}{\eta}\right) - k_2 |s|^{g+1}\right) \leq 0 \tag{5}$$

Thus, the stability condition can be guaranteed.

Case 1: Assuming $s(0) > 1$, the reaching process can be divided into two stages: $s(0) \to s = 1$ and $s = 1 \to s = 0$.

For the first stage, $s(0) \to s = 1$, (3) can be written as:

$$\dot{s} = -k_3 \tanh\left(\frac{s}{\eta}\right) - k_2 s^r \tag{6}$$

Hence, the convergence time can be determined as:

$$\begin{aligned}\int_0^{t_1} dt &= \int_1^{s(0)} \frac{1}{k_3 \tanh\left(\frac{s}{\eta}\right) + k_2 s^r} ds \\ &< \int_1^{s(0)} \frac{1}{k_2 s^r} ds = \frac{s(0)^{1-r} - 1}{(1-r)k_2}\end{aligned} \tag{7}$$

For the second stage, $s = 1 \to s = 0$, (3) can be written as:

$$\dot{s} = -k_3 \tanh\left(\frac{s}{\eta}\right) - k_2 s \tag{8}$$

In practice, s may only approach a value near zero and we assume that the slope of this value is small enough, e.g., 0.001, 0.0001, etc. In this case, there may be a small steady-state error but it probably will not influence the convergence precision of the system. We define the convergence value as equal to σ approaching zero. Thus, the convergence time can be calculated as:

$$\int_0^{t_2} dt = \int_\sigma^1 \frac{1}{k_3 \tanh\left(\frac{s}{\eta}\right) + k_2 s} ds < \int_\sigma^1 \frac{1}{k_2 s} ds = -\frac{\ln(\sigma)}{k_2} \tag{9}$$

Hence, the total time t_1^s can be calculated as:

$$t_1^s = t_1 + t_2 < \frac{1 - s(0)^{1-r}}{(r-1)k_2} - \frac{\ln(\sigma)}{k_2} \tag{10}$$

Case 2: Assuming $s(0) < -1$, the reaching manner also has two stages: from $s(0) \to s = -1$ and from $s = -1 \to s = 0$. The analysis in this case is similar to that of Case 1. Thus, the sum time t_2^s can be calculated as:

$$t_2^s < \frac{1 - (-s(0))^{1-r}}{(r-1)k_2} - \frac{\ln(\sigma)}{k_2} \tag{11}$$

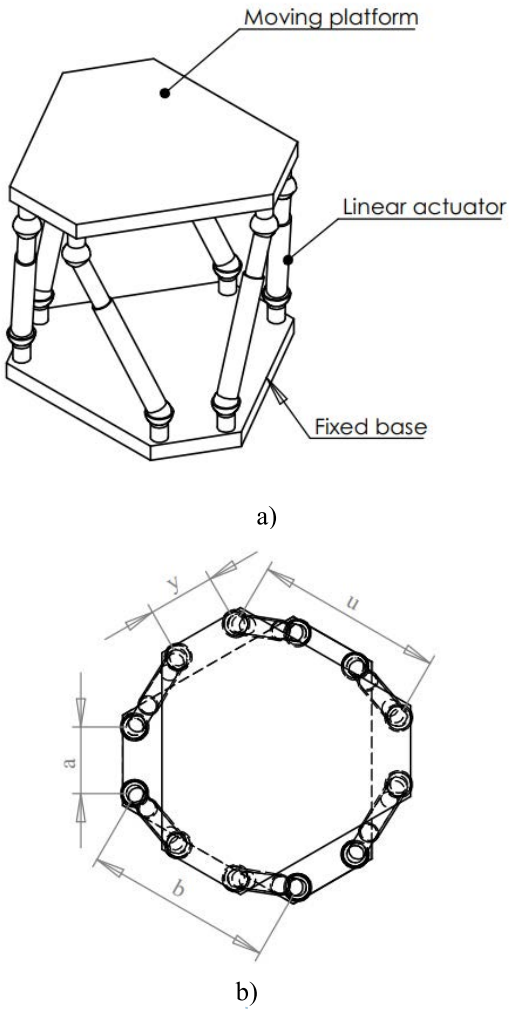

FIGURE 3. a) The SP; b) top view.

Overall, the sliding mode s can reach the value approaching 0 in a finite time t^s for any initial condition $s(0)$:

$$t^s < \frac{1 - |s(0)|^{1-r}}{(r-1)k_2} - \frac{\ln(\sigma)}{k_2} \tag{12}$$

III. STEWART PLATFORM DYNAMIC

Figure 3 shows a SP mainly constructed of six linear actuators, a fixed base, and a moving platform. The kinematics and dynamics of the SP were studied in much previous research [11]–[14]. We assume that the position of the center of the moving platform is $[p_x, p_y, p_z]$ with respect to a coordinate {O} placed at the center of the fixed base, and the orientation of the moving platform is described by a rotation of angle φ_x about the x-axis of {O} (roll), then about the y-axis of {O} by angle φ_y (pitch) and about the z-axis of {O} by angle φ_z (yaw). Generally, the dynamic equation of the SP can be given as follows:

$$F = J^T \tau = M(X)\ddot{X} + C(X, \dot{X})\dot{X} + G(X) + f_d \tag{13}$$

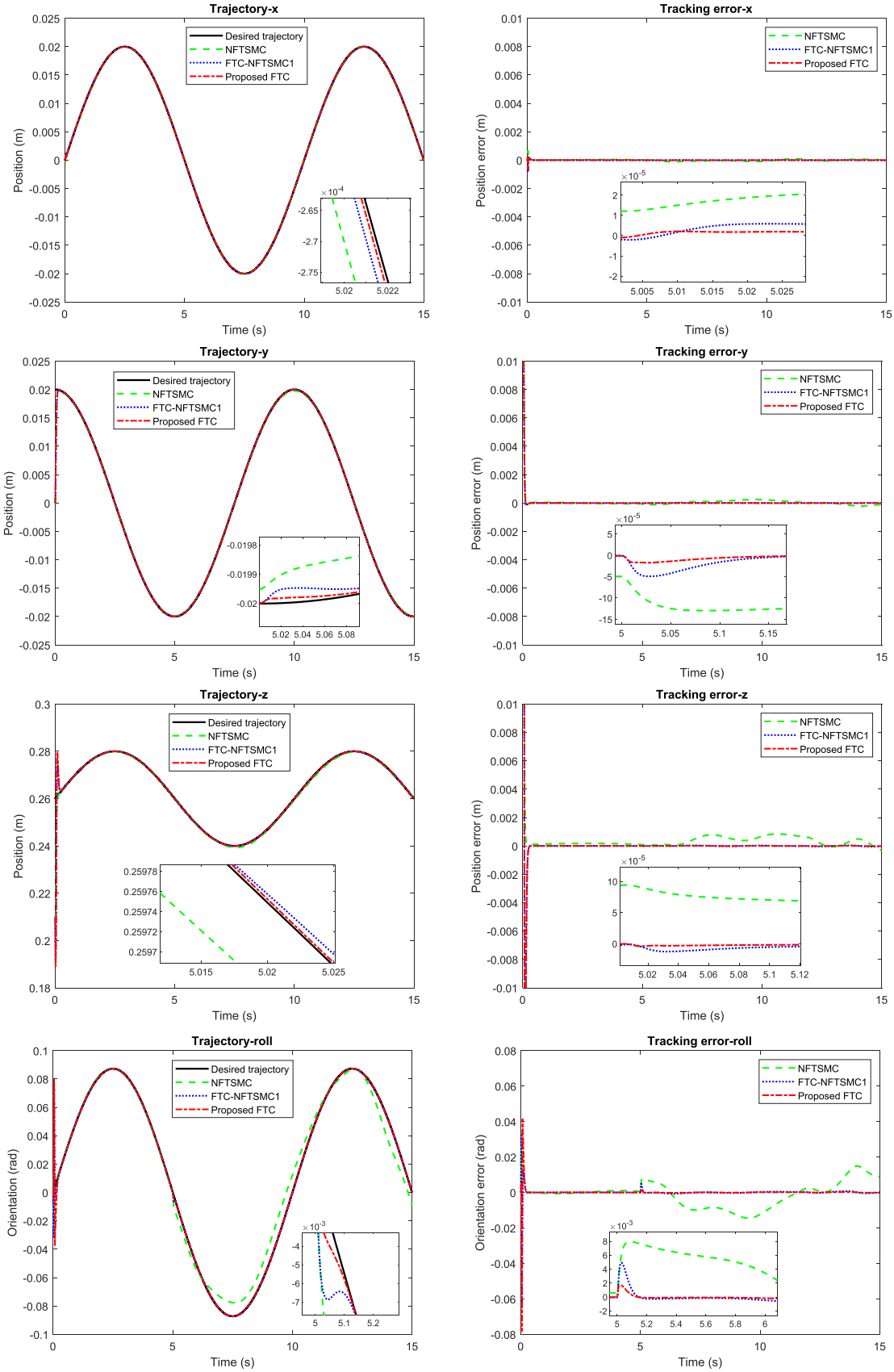

FIGURE 4. The tracking trajectory and performance of NFTSMC, FTC-NFTSMC1, and Proposed FTC for the SP.

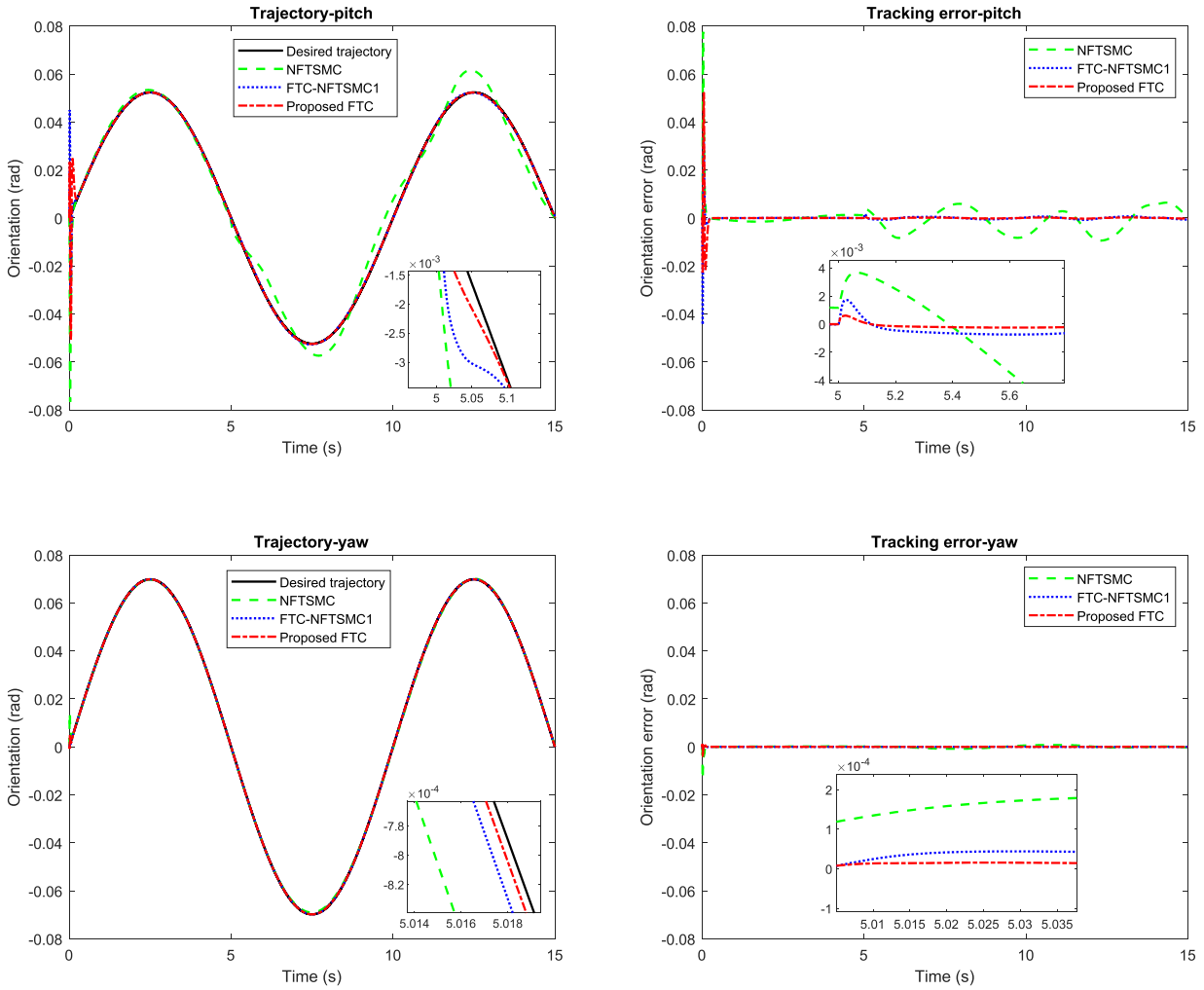

FIGURE 4. ***(Continued.)*** **The tracking trajectory and performance of NFTSMC, FTC-NFTSMC1, and Proposed FTC for the SP.**

where $\tau \in R^6$ is the vector of the force of the actuator, J is a Jacobian matrix, F is the vector of force in Cartesian space, $M(X)$ is an inertia matrix, $C(X, \dot{X})$ is the matrix of Coriolis/centrifugal force, $G(X)$ is the vector of gravitation force, f_d is the unknown disturbance of the system, and $X = [p_x, p_y, p_z, \varphi_x, \varphi_y, \varphi_z]^T$.

The uncertainties of the system dynamics can be expressed as nominal and deviational as follows:

$$M = M_o + \Delta M, \quad C = C_o + \Delta C, \quad G = G_o + \Delta G$$

where M_o, C_o, and G_o are the nominal model dynamics and ΔM, ΔC, ΔG are unknown model uncertainties. (13) can be rewritten as:

$$F = J^T \tau = M_o \ddot{X} + C_o \dot{X} + G_o + \Psi \tag{14}$$

where $\Psi = \Delta M.\ddot{X} + \Delta C.\dot{X} + \Delta G + f_d$.

However, in practice there are certain faults, such as sensor faults, mechanical faults, and actuator faults. In this paper, we consider actuator faults.

According to Li and Tong [35], actuator faults can be divided into bias fault and gain fault. The actuator fault model can be written as:

$$\tau_i^f = (1 - \rho_i(t))\tau_i + f_i(t)\ (t > t_f), \quad i = 1, 2, \ldots, n \tag{15}$$

where $f_i(t)$ denotes a bounded signal (bounded function) and $\rho_i(t)$ is the unknown remaining control rate, $0 \leq \rho_i(t) \leq 1$. τ_i^f denotes the force of the ith actuator when the fault occurs, and t_f is the time of occurrence of the fault.

In general, the input vector of the SP can be written as:

$$\tau^f = (I - \rho(t))\tau + f(t) \tag{16}$$

where $\tau^f = \left[\tau_1^f, \tau_2^f, \ldots, \tau_6^f\right]^T$, $\rho = diag\{\rho_1, \rho_2, \ldots, \rho_6\}$, $f = [f_1, f_2, \ldots, f_6]^T$, and I is an identity matrix 6×6.

Substituting (16) into (14) yields:

$$\ddot{X} = M_o^{-1}\zeta - M_o^{-1}\left(J^T\rho(t)\tau - J^T f(t) + \Psi\right) \tag{17}$$

where $\zeta = F - C_o\dot{X} - G_o$

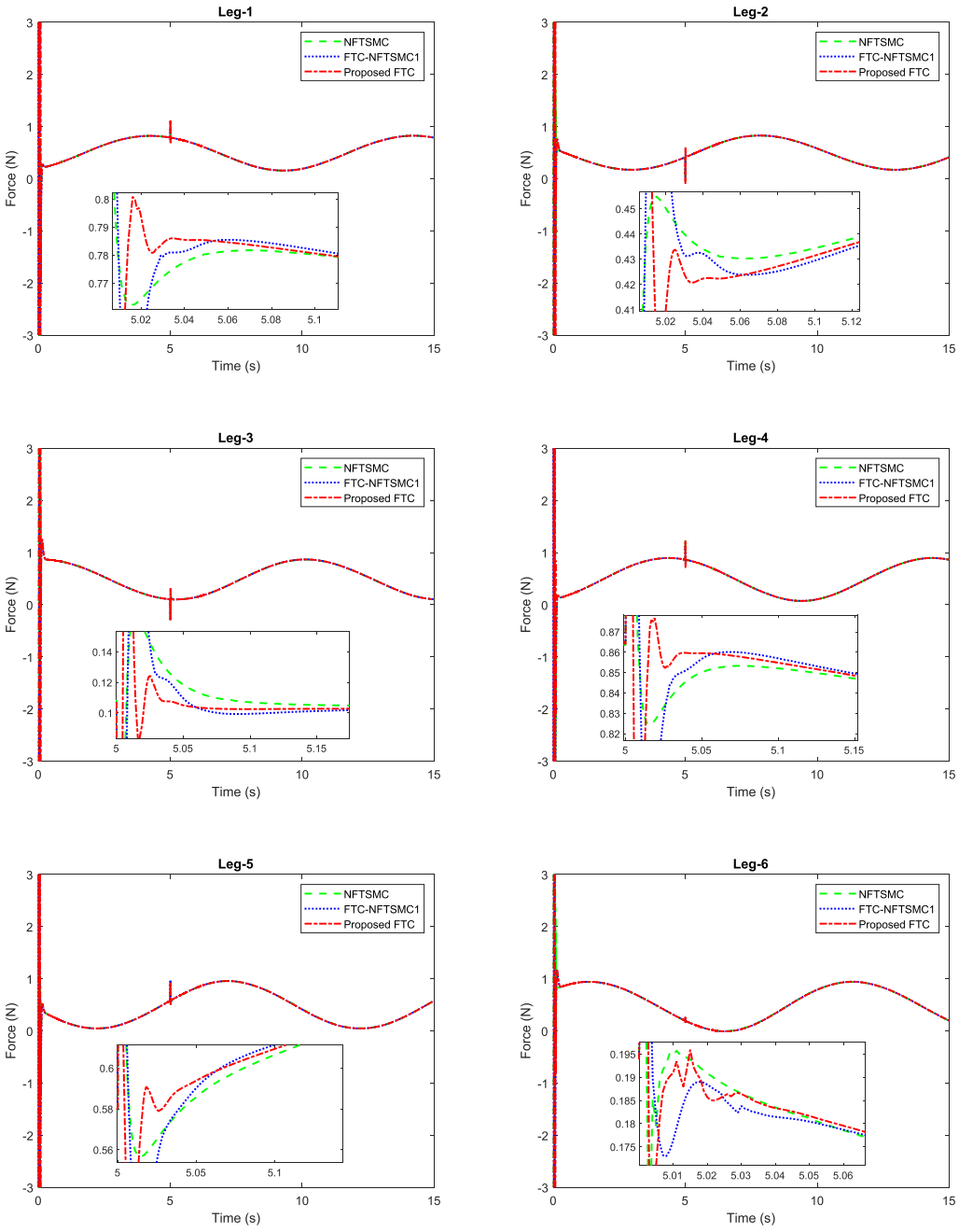

FIGURE 5. Input force at each leg of the SP for NFTSMC, FTC-NFTSMC1, and Proposed FTC.

IV. THE EXTENDED STATE OBSERVER FOR ESTIMATION OF THE UNCERTAINTY, DISTURBANCE, AND FAULT

The dynamic model (17) can be rewritten in the state space as follows:

$$\begin{cases} \dot{x}_1 = x_2 \\ \dot{x}_2 = M_o^{-1}\zeta - M_o^{-1}\left(J^T\rho(t)\tau - J^T f(t) + \Psi\right) \end{cases} \tag{18}$$

where $x_1 = X \in R^6, x_2 = \dot{X} \in R^6$.

We define $x_3 \triangleq -M_o^{-1}\left(J^T\rho(t)\tau - J^T f(t) + \Psi\right)$ to be the extended state of the system (18), then (18) becomes:

$$\begin{cases} \dot{x}_1 = x_2 \\ \dot{x}_2 = M_0^{-1}\zeta + x_3 \end{cases} \tag{19}$$

According to [34], a conventional linear ESO can be designed as:

$$\begin{cases} \dot{\widehat{x}}_1 = \widehat{x}_2 + \frac{\alpha_1}{\mu}\left(x_1 - \widehat{x}_1\right) \\ \dot{\widehat{x}}_2 = M_o^{-1}\zeta + \frac{\alpha_2}{\mu^2}\left(x_1 - \widehat{x}_1\right) + \widehat{x}_3 \\ \dot{\widehat{x}}_3 = \frac{\alpha_3}{\mu^3}\left(x_1 - \widehat{x}_1\right) \end{cases} \tag{20}$$

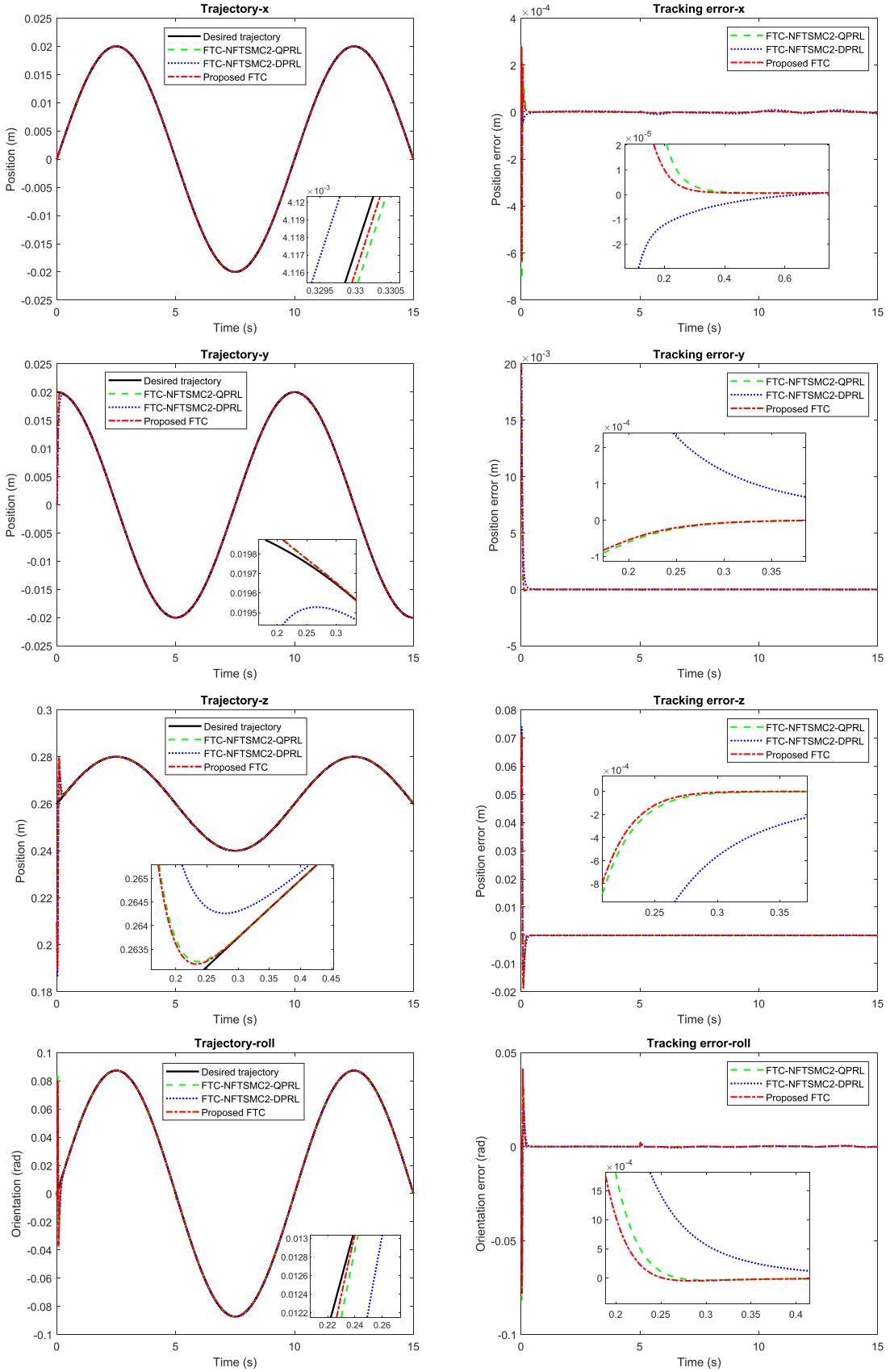

FIGURE 6. The tracking trajectory and performance of FTC-NFTSMC2-QPRL, FTC-NFTSMC2-DPRL, and Proposed FTC for the SP.

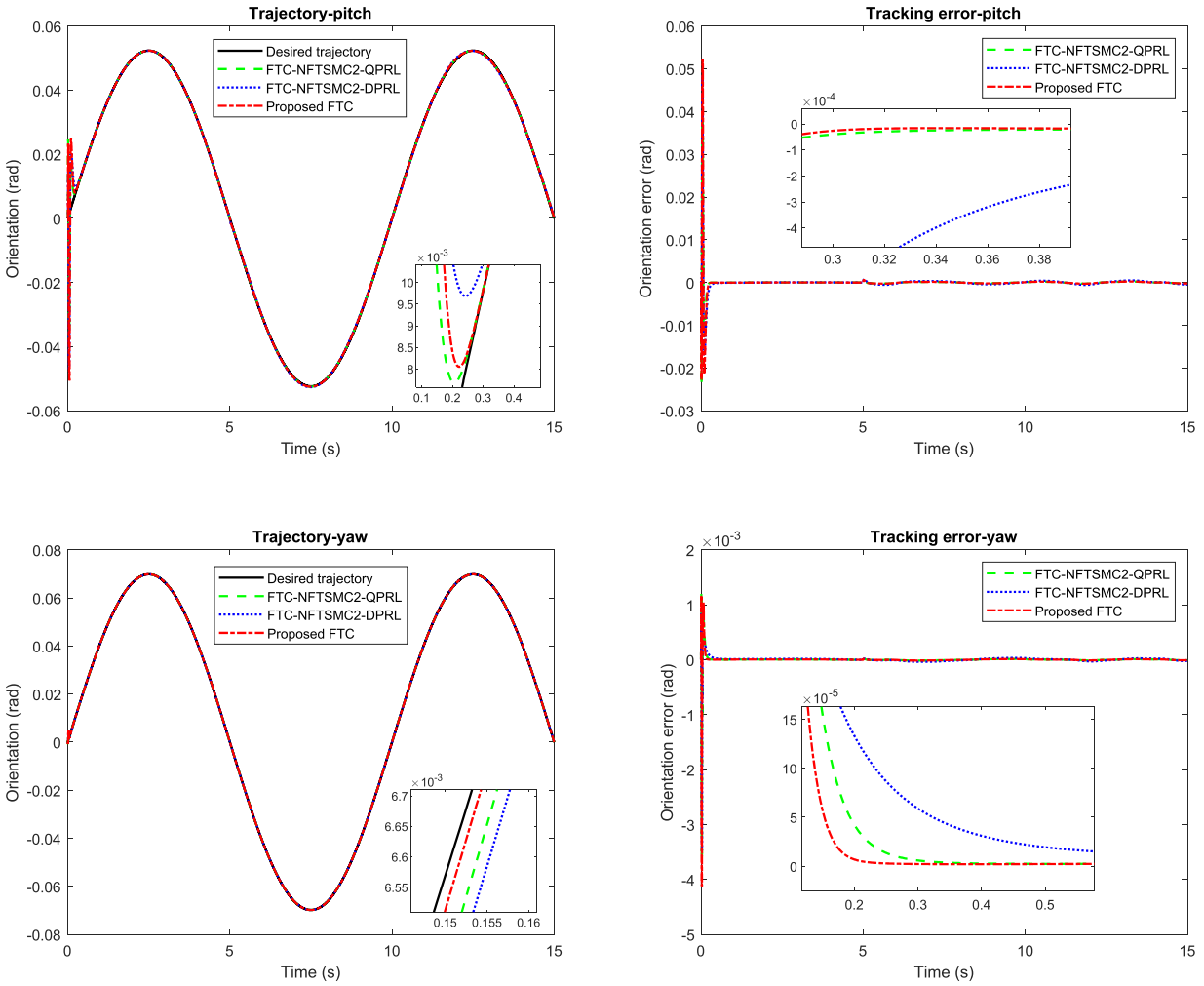

FIGURE 6. *(Continued.)* **The tracking trajectory and performance of FTC-NFTSMC2-QPRL, FTC-NFTSMC2-DPRL, and Proposed FTC for the SP.**

where $\widehat{x}_1, \widehat{x}_2, \widehat{x}_3$ are observer states, $\alpha_1, \alpha_2, \alpha_3$ are positive constants chosen so that the polynomial $s^3 + \alpha_1 s^2 + \alpha_2 s + \alpha_3$ is a Hurwitz polynomial, and $\mu < 1$ is a small positive constant.

As aforementioned, some disadvantages of the conventional ESO (20) (ESO1) are the peaking issue and high sensitivity to measurement noise. Hence, a different ESO is proposed by Ran *et al.* [24] to decrease the influence of these downsides on the system, and it can be described as:

$$\begin{cases} \dot{\phi}_1 = \dfrac{\alpha_1}{\mu}(x_1 - \phi_1), & \widehat{x}_2 = \dfrac{\alpha_1}{\mu}(x_1 - \phi_1) \\ \dot{\phi}_2 = M_o^{-1}\zeta + \dfrac{\alpha_2}{\mu}\left(\widehat{x}_2 - \phi_2\right), & \widehat{x}_3 = \dfrac{\alpha_2}{\mu}\left(\widehat{x}_2 - \phi_2\right) \end{cases} \tag{21}$$

where $\phi_1, \phi_2 \in R^6$, $0 < \mu < 1$ is a small positive constant, and α_1, α_2 are odd positive constants.

Ran *et al.* [24] demonstrated the convergence of the new ESO (21) (ESO2) such that there exists $\delta > 0$ and $T > 0$ such that:

$$\left|x_i(t) - \widehat{x}_i(t)\right| \leq \delta, \quad 2 \leq i \leq 3, \ \forall t \geq T.$$

V. DESIGN OF A FAULT-TOLERANT CONTROL

In this section, a fault-tolerant control based on NFTSMC, ESO2, and the improved reaching law (3) is developed for the SP. The sliding surface of the NFTSMC is defined as:

$$s = e + \lambda_1 e^{l/h} + \lambda_2 \dot{e}^{p/q} \tag{22}$$

where $e = X_d - X$. X_d is the desired trajectory in Cartesian space, l, h, p, and q are positive odd integers, $1 < p/q < 2$, $l/\mathrm{h} > p/q$, and λ_1 and λ_2 are the positive constants.

Taking the time derivative of (22) yields:

$$\dot{s} = \dot{e} + \lambda_1 \frac{l}{h} |e|^{\frac{l}{h}-1} \dot{e} + \lambda_2 \frac{p}{q} |\dot{e}|^{\frac{p}{q}-1} (\ddot{X}_d - \ddot{X}) \tag{23}$$

Substituting (19) into (23) yields:

$$\dot{s} = \dot{e} + \lambda_1 \frac{l}{h} |e|^{\frac{l}{h}-1} \dot{e} + \lambda_2 \frac{p}{q} |\dot{e}|^{\frac{p}{q}-1} \left(\ddot{X}_d - M_o^{-1}\zeta - x_3\right) \tag{24}$$

Applying ESO2 and the proposed reaching law (3) for control input, then the proposed FTC law is described as follows:

$$F = F_{eq} + F_s \tag{25}$$

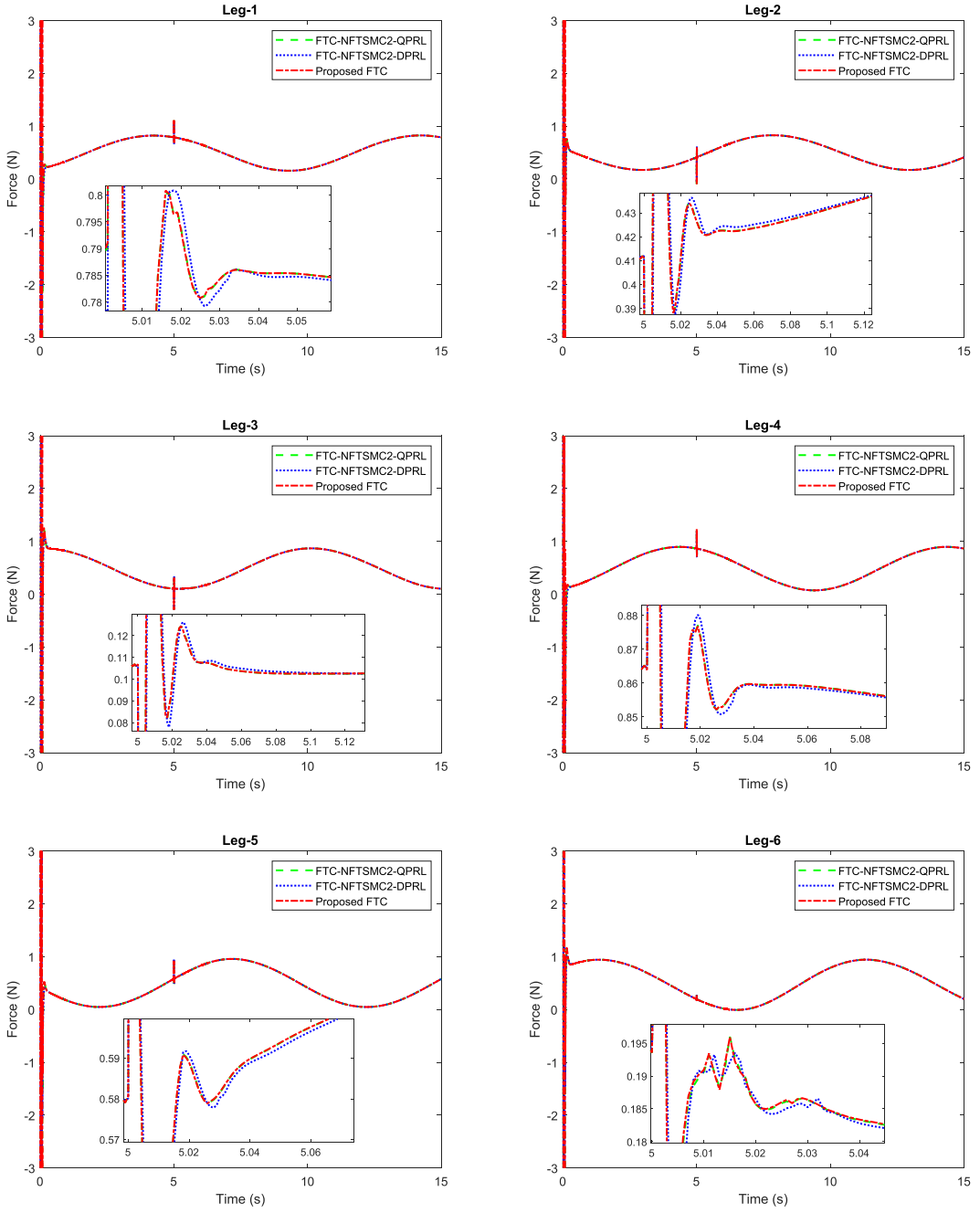

FIGURE 7. Input force at each leg of the SP for FTC-NFTSMC2-QPRL, FTC-NFTSMC2-DPRL, and Proposed FTC.

where

$$F_{eq} = M_o \begin{pmatrix} \ddot{X}_d + \dfrac{1}{\lambda_2}\dfrac{q}{p}\dot{e}^{2-\frac{p}{q}} \\ + \dfrac{\lambda_1}{\lambda_2}\dfrac{l}{h}\dfrac{q}{p}|e|^{\frac{l}{h}-1}\dot{e}^{2-\frac{p}{q}} - \widehat{x}_3 \\ + k_2|s|^g \operatorname{sgn}(s) \end{pmatrix} + C_o\dot{X} + G_o \tag{26}$$

is an equivalent control, and

$$F_s = M_o k_3 \tanh\left(\frac{s}{\eta}\right) \tag{27}$$

is a switching term

Theorem: Considering the SP described in (19) with the nonsingular fast terminal sliding surface defined in (22), the ESO in (21), the proposed reaching law in (3), and the FTC law designed in (25), then the tracking error e will converge to zero within a finite time.

Proof: Selecting a Lyapunov function as $V_2 = \frac{1}{2}s^2 \geq 0$ and taking the time derivative of V_2, we have:

$$\dot{V}_2 = s\dot{s} = s\begin{bmatrix} \dot{e} + \lambda_1\dfrac{l}{h}|e|^{\frac{l}{h}-1}\dot{e} \\ + \lambda_2\dfrac{p}{q}|\dot{e}|^{\frac{p}{q}-1}\left(\begin{matrix}\ddot{X}_d - M_o^{-1}\left(F - C_o\dot{X} - G_o\right) \\ - x_3\end{matrix}\right) \end{bmatrix} \tag{28}$$

FIGURE 8. 6-DOF actual SP.

Substituting (25) into (28), we have:

$$\dot{V}_2 = -\lambda_2 \frac{p}{q} k_3 s \left|\dot{e}\right|^{\frac{p}{q}-1} \tanh\left(\frac{s}{\eta}\right) - \lambda_2 k_2 \frac{p}{q} \left|\dot{e}\right|^{\frac{p}{q}-1} |s|^{g+1} + \lambda_2 \frac{p}{q} s \left|\dot{e}\right|^{\frac{p}{q}-1} (\widehat{x}_3 - x_3) \quad (29)$$

$$\dot{V}_2 \leq -\lambda_2 \frac{p}{q} k_3 s \left|\dot{e}\right|^{\frac{p}{q}-1} \tanh\left(\frac{s}{\eta}\right) - \lambda_2 \frac{p}{q} |s| \left|\dot{e}\right|^{\frac{p}{q}-1} \left(k_2 |s|^g - \delta\right) \quad (30)$$

Since $\lambda_2 \frac{p}{q} k_3 s \left|\dot{e}\right|^{\frac{p}{q}-1} \tanh\left(\frac{s}{\eta}\right) \geq 0$, to ensure that the system is stable, it needs to satisfy the condition as:

$$k_2 |s|^g \geq \delta \quad (31)$$

That means:

$$|s| \geq \left(\frac{\delta}{k_2}\right)^{1/g} \quad (32)$$

When $|s| \leq 1$, it leads to:

$$|s| \geq \frac{\delta}{k_2} \quad (33)$$

This implies that the states of the system can converge in a finite time and δ/k_2 is a convergence region of the sliding mode variable s.

The finite time t_s of (22) is the traveling time from $e(t_r)$ to $e(t_r + t_s)$ introduced in [5] as:

$$t_s = \frac{\frac{p}{q} |e(0)|^{1-q/p}}{\lambda_1 \left(\frac{p}{q} - 1\right)} \times H\left(\frac{q}{p}, \frac{\frac{p}{q}-1}{\left(\frac{l}{h}-1\right)\frac{p}{q}}; 1 + \frac{\frac{p}{q}-1}{\left(\frac{l}{h}-1\right)\frac{p}{q}}; -\lambda_1 |e(0)|^{l/h-1}\right) \quad (34)$$

where H denotes Gauss' hypergeometric function.

VI. SIMULATION RESULTS

To demonstrate the effectiveness of the proposed FTC, the simulation results are illustrated in this section. First, the mechanical model of the SP was designed in SolidWorks. Next, it was exported to the Simulink environment via the Simscape Multibody link tool, and the simulation was executed in MATLAB/Simulink. The parameters of the SP $a, b, y, u, m_p, I_{xx}, I_{yy}$, and I_{zz} were given in SolidWorks as 54 mm, 198 mm, 54 mm, 126 mm, 145 g, 296,223 g.mm^2, 296,223 g.mm^2, and 588,962 g.mm^2, respectively.

The reference trajectory of the moving platform was described according to the following expression:

$$X_d = \begin{bmatrix} 0.02\sin(0.2\pi t)\ (m) \\ 0.02\cos(0.2\pi t)\ (m) \\ 0.26 + 0.02\sin(0.2\pi t)\ (m) \\ \frac{\pi}{36}\sin(0.2\pi t)\ (rad) \\ \frac{\pi}{60}\sin(0.2\pi t)\ (rad) \\ \frac{\pi}{45}\sin(0.2\pi t)\ (rad) \end{bmatrix} \quad (35)$$

First, the performance of the proposed FTC with the ESO2 was compared to the FTC with the conventional ESO1 and the NFTSMC without the ESO. The control input of the NFTSMC can be given as:

$$F = M_o \begin{pmatrix} \ddot{X}_d + \frac{1}{\lambda_2}\frac{q}{p}\dot{e}^{2-\frac{p}{q}} \\ + \frac{\lambda_1}{\lambda_2}\frac{l}{h}\frac{q}{p} e^{\frac{l}{h}-1}\dot{e}^{2-\frac{p}{q}} \\ + k_3 \tanh\left(\frac{s}{\eta}\right) + k_2 |s|^g \operatorname{sgn}(s) \end{pmatrix} + C_o\dot{X} + G_o \quad (36)$$

The control parameters in (36) and (25) were selected as $\lambda_1 = 0.1, \lambda_2 = 0.02, l = 27, h = 19, q = 19, p = 21, k_1 = 5, k_2 = 2,000, \varepsilon = 0.1, c = 0.2, \eta = 0.1$, and $r = 1.1$. The parameters of the ESO1 were given as $\alpha_1 = 3, \alpha_2 = 3, \alpha_3 = 1$, and $\mu = 0.005$. For the ESO2, the parameters were set as $\alpha_1 = 1, \alpha_2 = 1, \mu = 0.005$. The disturbance of the system was assumed as $f_d = 0.01\sin(t)$. It could be assumed that multiple faults arose at the first, third, and fifth actuators at 5 sec. The torque functions with multiple faults were given in (16), where $\rho_1(t) = 0.3 + 0.2\cos(\pi t), \rho_2(t) = 0, \rho_3(t) = 0.2 + 0.2\sin(t), \rho_4(t) = 0, \rho_5(t) = 0.2 + 0.1\sin(2t), \rho_6(t) = 0, f_1(t) = 0.1\sin(t), f_2(t) = 0, f_3(t) = 0.5\cos(2t), f_4(t) = 0, f_5(t) = \cos(0.5t)$, and $f_6(t) = 0$.

Figure 4 shows the tracking trajectory and performance of a NFTSMC without ESO (NFTSMC), a FTC using the conventional ESO1 (FTC-NFTSMC1), and the proposed FTC (25) using ESO2 (Proposed FTC). When the faults did not occur in the first 5 sec, the tracking performances of controllers were almost the same. However, the performances of the controllers significantly changed after the faults appeared. As shown, the FTC-NFTSMC1 and Proposed FTC had more excellent performance than the NFTSMC because the faults were efficiently estimated and compensated by ESO1 and

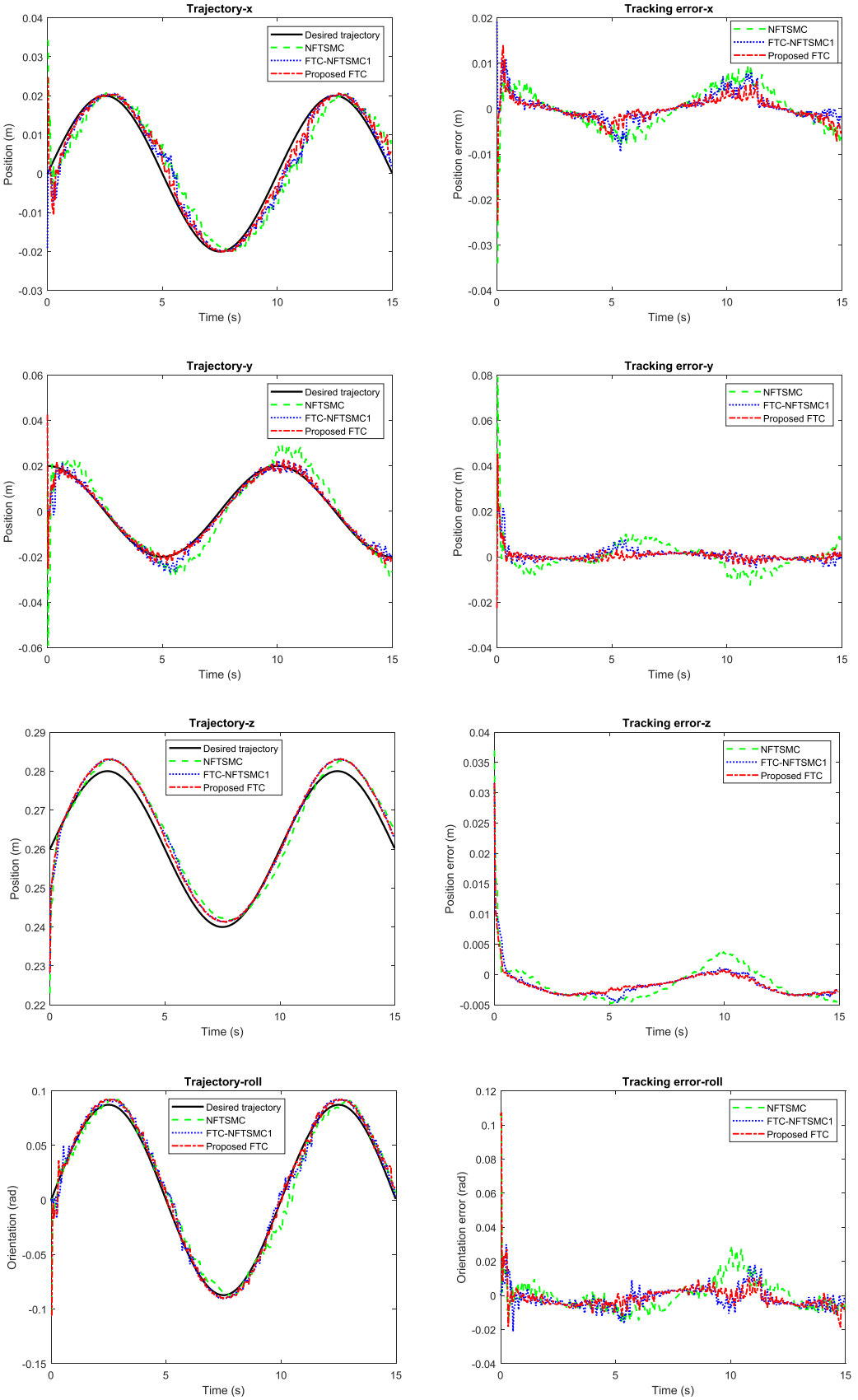

FIGURE 9. The tracking trajectory and performance of NFTSMC, FTC-NFTSMC1, and Proposed FTC for the actual SP.

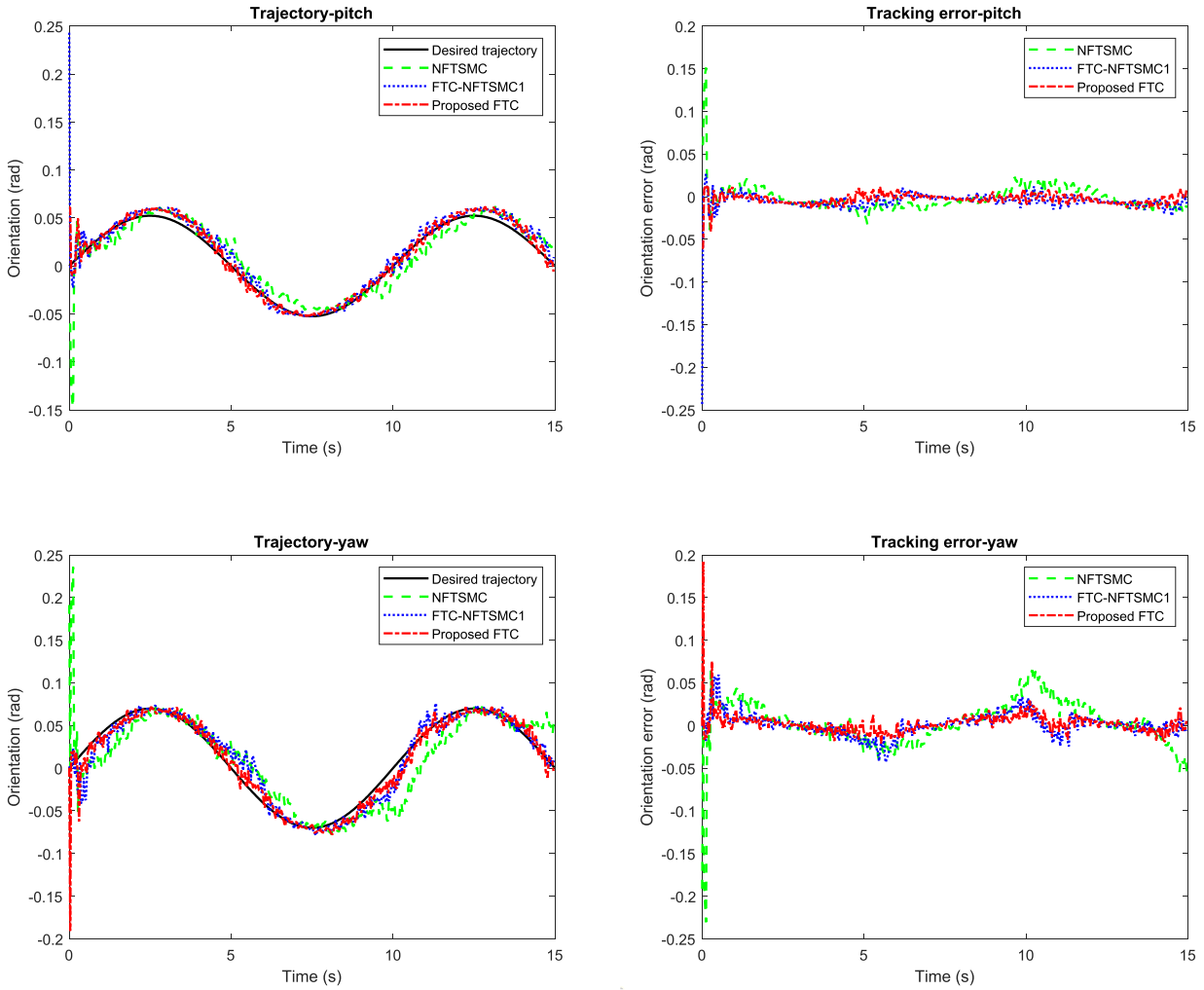

FIGURE 9. *(Continued.)* **The tracking trajectory and performance of NFTSMC, FTC-NFTSMC1, and Proposed FTC for the actual SP.**

ESO2. Furthermore, Proposed FTC had less peaking than did FTC-NFTSMC1 and NFTSMC. This exhibits the success in lessening the peaking value of ESO2 in the proposed FTC compared to that of the conventional ESO1.

Next, to verify the effectiveness of the improved reaching law, the performance of the proposed FTC law (25) using the NRL (3) (Proposed FTC) was compared with that of the FTC laws using the QPRL (FTC-NFTSMC2-QPRL) and the DPRL (FTC-NFTSMC2-DPRL) respectively described as:

$$F = M_o \left(\begin{array}{l} \ddot{X}_d + \dfrac{1}{\lambda_2}\dfrac{q}{p}\dot{e}^{2-\frac{p}{q}} \\ +\dfrac{\lambda_1}{\lambda_2}\dfrac{l}{h}\dfrac{q}{p}e^{\frac{l}{h}-1}\dot{e}^{2-\frac{p}{q}} - \widehat{x}_3 \\ +k_1 |s|^{w_1} \operatorname{sgn}(s) + k_2 s \end{array} \right) + C_o\dot{X} + G_o \qquad (37)$$

$$F = M_o \left(\begin{array}{l} \ddot{X}_d + \dfrac{1}{\lambda_2}\dfrac{q}{p}\dot{e}^{2-\frac{p}{q}} \\ +\dfrac{\lambda_1}{\lambda_2}\dfrac{l}{h}\dfrac{q}{p}e^{\frac{l}{h}-1}\dot{e}^{2-\frac{p}{q}} - \widehat{x}_3 \\ +k_1 |s|^{w_1} \operatorname{sgn}(s) + k_2 |s|^{w_2} \operatorname{sgn}(s) \end{array} \right) + C_o\dot{X} + G_o \qquad (38)$$

Proposed FTC, FTC-NFTSMC2-QPRL, and FTC-NFTSMC2-DPRL use the same ESO2. The parameters in (37) and (38) are given as $\lambda_1 = 0.1, \lambda_2 = 0.02, l = 27, h = 19, q = 19, p = 21, k_1 = 5, k_2 = 2,000, w_1 = 0.8$, and $w_2 = 1.1$. The tracking performances of the three controllers are shown in Figure 6. As we can see, the convergence speed of Proposed FTC was faster than that of FTC-NFTSMC2-QPRL and FTC-NFTSMC2-DPRL. Besides, all three controllers had good tracking errors in the presence of the actuator faults, which demonstrates the efficiency of ESO2 compensating the faults regardless of which reaching law was used in the FTC law. In addition, when the faults occurred, Proposed FTC and FTC-NFTSMC2-QPRL had slightly better performance than FTC-NFTSMC2-DPRL because the convergence speed of FTC-NFTSMC2-DPRL was slightly slower than the other two when the system states changed around the sliding surface, as mentioned in Section II. Therefore, the proposed FTC scheme had not only a fast transient response but also robustness to the lumped uncertainty and faults of the system and the decrease of the peaking value. The control signals of all controllers are illustrated in Figures 5 and 7.

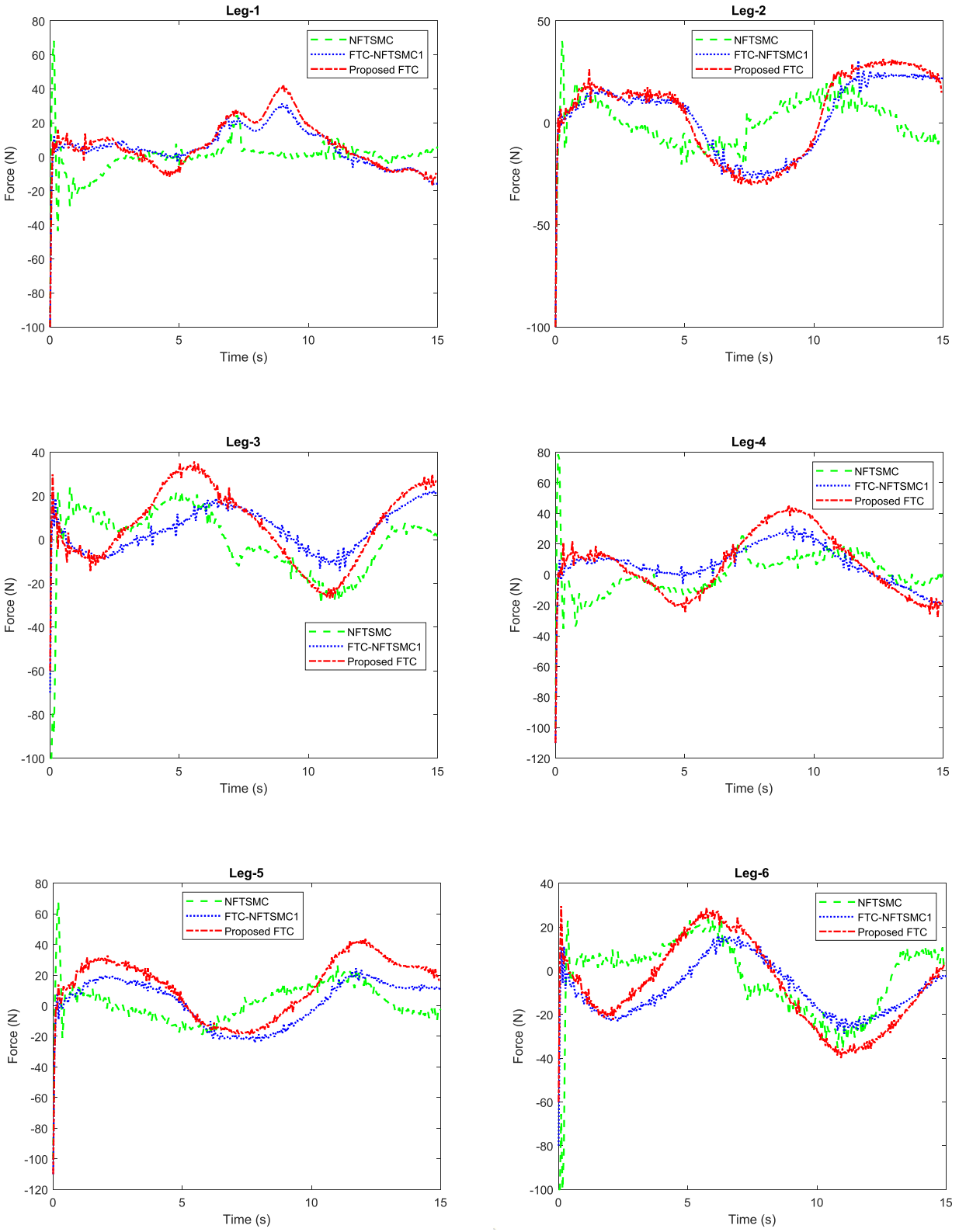

FIGURE 10. Input force at each leg of the actual SP for NFTSMC, FTC-NFTSMC1, and Proposed FTC.

VII. EXPERIMENTAL RESULTS

This section describes implementations of the proposed FTC compared with the other controllers for an actual SP that was assembled with plastic upper and lower platforms and six MightyZap actuators (12Lf-17F-90; IR Robot Co., Ltd., Korea). This actual SP in Figure 8 was designed with

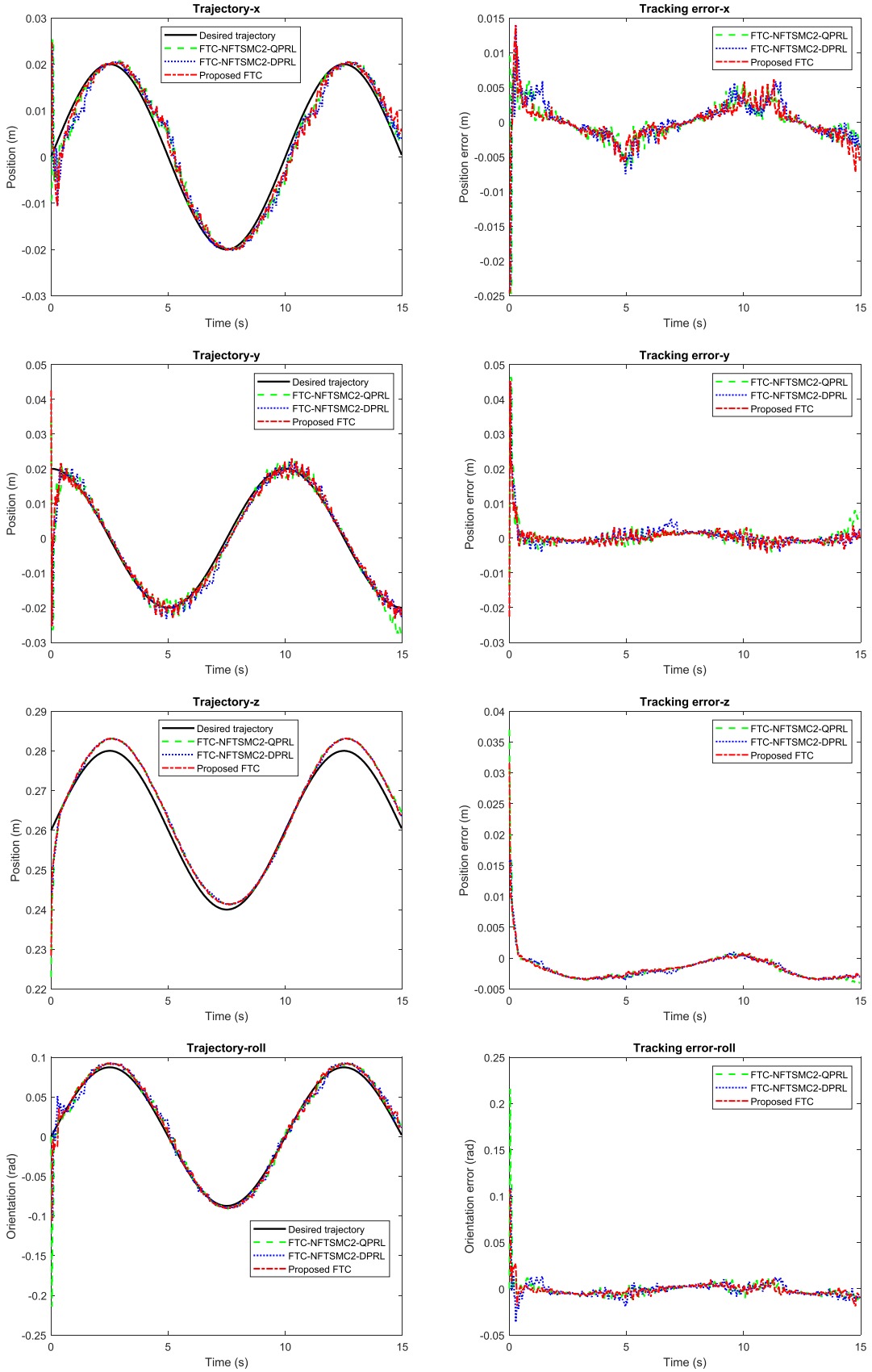

FIGURE 11. The tracking trajectory and performance of FTC-NFTSMC2-QPRL, FTC-NFTSMC2-DPRL, and Proposed FTC for the actual SP.

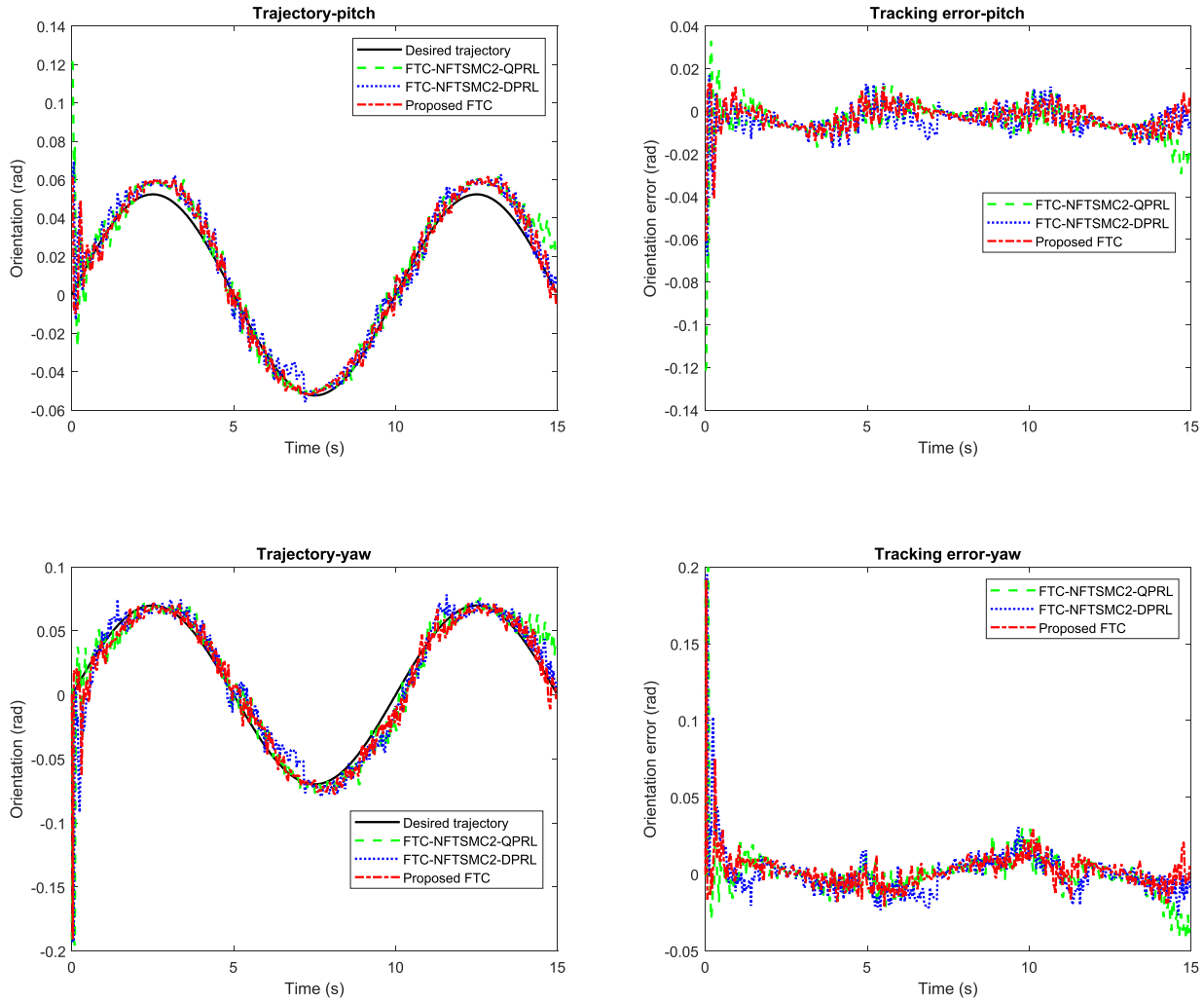

FIGURE 11. ***(Continued.)*** **The tracking trajectory and performance of FTC-NFTSMC2-QPRL, FTC-NFTSMC2-DPRL, and Proposed FTC for the actual SP.**

parameters a, b, y, and u set as 54 mm, 198 mm, 54 mm, and 126 mm, respectively. The reference trajectory of the upper platform was given in (35). The parameters in the FTC law (25) and the NFTSMC (36) were set as $\lambda_1 = 0.1$, $\lambda_2 = 0.02$, $l = 27$, $h = 19$, $q = 19$, $p = 21$, $k_1 = 0.1$, $k_2 = 400$, $\varepsilon = 0.1$, $c = 0.2$, $\eta = 0.1$, and r = 1.1. For the conventional ESO1, the parameters are given as $\alpha_1 = 3$, $\alpha_2 = 3$, $\alpha_3 = 1$, and $\mu = 0.09$. The ESO2 was designed with the parameters $\alpha_1 = 1$, $\alpha_2 = 1$, and $\mu = 0.09$.

Next, we assumed that multiple faults occurred in the first, third, and fifth actuators at 5 sec, as described in the Simulation section (VI above), and the torque functions with multiple faults were described in (16) where the parameters were set as in the Simulation section.

The tracking trajectory and performance of the NFTSMC, FTC-NFTSMC1, and Proposed FTC are illustrated in Figure 9. The performances of FTC-NFTSMC1 and Proposed FTC were slightly better than that of NFTSMC within the first 5 sec. When actuator faults appeared after 5 sec, the tracking errors of FTC-NFTSMC1 and Proposed FTC were considerably lower than those of NFTSMC due to the successful compensation of ESO1 and ESO2 for the disturbances, uncertainties, and faults. In addition, the peaking value in Proposed FTC was a little lower than that of FTC-NFTSMC1 when the fault occurred. It should be noted that the actual SP might have had different uncertainty and disturbance compared to the simulation, so the performance results of the actual SP were unlike those of the simulation. Overall, FTC-NFTSMC1 and Proposed FTC had smaller tracking errors than NFTSMC, while Proposed FTC achieved slightly higher accuracy than FTC-NFTSMC1. Figure 10 shows the control signals of three controllers. FTC-NFTSMC1 and Proposed FTC use ESO1 and ESO2 respectively to compensate for uncertainties, disturbances, and faults, while NFTSMC has no compensation for those. Hence, the controllers gave major differences in the input force at each joint.

To evaluate the efficiency of the proposed reaching law, we investigated the performance of FTC-NFTSMC2-QPRL (37), FTC-NFTSMC2-DPRL (38), and our Proposed FTC (25) in controlling the actual SP. The parameters in (37)

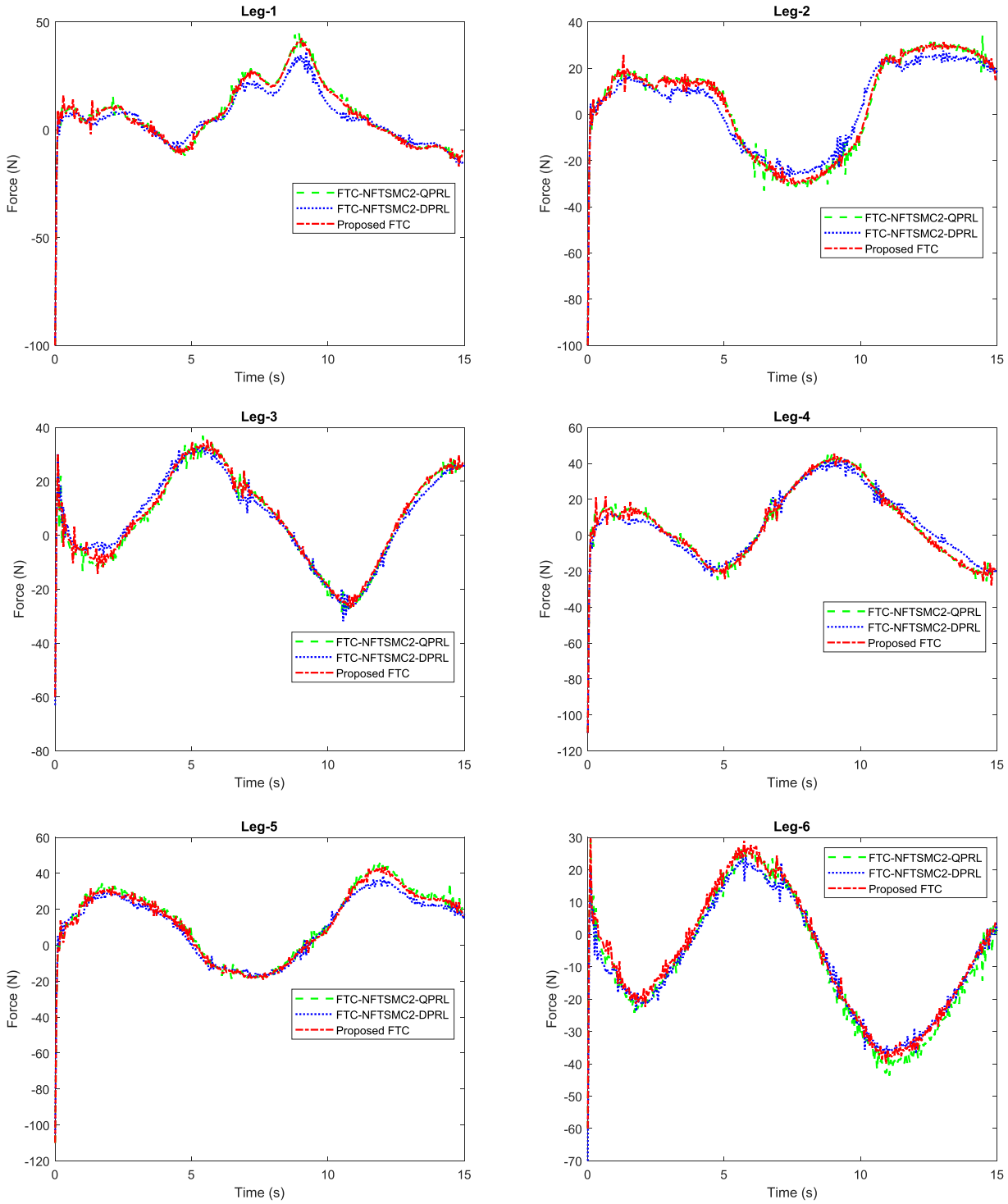

FIGURE 12. Input force at each leg of the actual SP for FTC-NFTSMC2-QPRL, FTC-NFTSMC2-DPRL, and Proposed FTC.

and (38) are given as $\lambda_1 = 0.1$, $\lambda_2 = 0.02$, $l = 27$, $h = 19$, $q = 19$, $p = 21$, $k_1 = 5$, $k_2 = 400$, $w_1 = 0.8$, and $w_2 = 1.1$. Figure 11 illustrates the trajectory and performance of Proposed FTC compared with FTC-NFTSMC2-QPRL and FTC-NFTSMC2-DPRL. In general, the three controllers had similar performances in the presence of the actuator faults. Also, due to possible limitations of the hardware, it was not as easy to clearly see the difference in the convergence speed of the controllers as it had been in the simulation. The three controllers use the same ESO2 for the estimation

and compensation, thus there were no significant differences in the magnitude of control signals at each leg shown in Figure 12.

VIII. CONCLUSION

In this paper, a new fault-tolerant scheme was proposed for a Stewart platform. First, a NFTSMC was used in the FTC to enhance the convergence speed of the state in finite time without the singularity issue. Then ESO2 was applied for the FTC to not only effectively estimate and compensate for uncertainties, disturbances and faults, but also reduce the peaking issue in the conventional ESO1. To further enhance the reaching phase speed and decrease the chattering, an improved reaching law (3) was designed and its quick convergence ability in finite time was demonstrated. Consequently, the new FTC showing the above benefits was derived by combining the NFTSMC, the ESO2 and the novel reaching law (3). To assess the efficiency of the proposed FTC, the desired trajectory and an assumption of faults were used for all the controllers throughout the simulation and experiments. Next, we showed a comparison between the proposed FTC and the control law using the traditional ESO1 and the control law without the ESO to evaluate the effectiveness of ESO2 in the FTC scheme. Then, the performance of the proposed FTC and the other FTC schemes using the same ESO2 but different reaching laws are exhibited to demonstrate enhancement in the convergence rate of the NRL. By verifying the simulation and the experiments, we could confirm that the proposed FTC is easy to implement and has the inherent advantages of the NFTSMC, the estimation and compensation ability of ESO2 plus the reaching speed improvement of the improved reaching law (3). Thus, the proposed FTC showed remarkable features such as insensitivity to uncertainties, disturbances, and faults, reducing the peaking value, high precision and robustness, rejecting the singularity, less oscillation, and a fast convergence speed in finite time.

REFERENCES

[1] J.-J.-E. Slotine and W. Li, "On the adaptive control of robot manipulators," *Int. J. Robot. Res.*, vol. 6, no. 3, pp. 49–59, Sep. 1987, doi: 10.1177/027836498700600303.

[2] Q. Meng, T. Zhang, X. Gao, and J.-Y. Song, "Adaptive sliding mode fault-tolerant control of the uncertain Stewart platform based on offline multibody dynamics," *IEEE/ASME Trans. Mechatronics*, vol. 19, no. 3, pp. 882–894, Jun. 2014, doi: 10.1109/TMECH.2013.2262527.

[3] S. Lin and A. A. Goldenberg, "Neural-network control of mobile manipulators," *IEEE Trans. Neural Netw.*, vol. 12, no. 5, pp. 1121–1133, Sep. 2001, doi: 10.1109/72.950141.

[4] J. Ma, T. Yang, Z.-G. Hou, and M. Tan, "Neural network disturbance observer based controller of an electrically driven Stewart platform using backstepping for active vibration isolation," in *Proc. Int. Joint Conf. Neural Netw.*, Jun. 2009, pp. 1939–1944, doi: 10.1109/IJCNN.2009.5179041.

[5] L. Yang and J. Yang, "Nonsingular fast terminal sliding-mode control for nonlinear dynamical systems," *Int. J. Robust Nonlinear Control*, vol. 21, no. 16, pp. 1865–1879, 2011, doi: 10.1002/rnc.1666.

[6] S. S. D. Xu, C. C. Chen, and Z. L. Wu, "Study of nonsingular fast terminal sliding-mode fault-tolerant control," *IEEE Trans. Ind. Electron.*, vol. 62, no. 6, pp. 3906–3913, Jun. 2015, doi: 10.1109/TIE.2015.2399397.

[7] W. Qiang, C. Juan, and T. Zhiyong, "Study of sliding mode control for Stewart platform based on simplified dynamic model," in *Proc. 6th IEEE Int. Conf. Ind. Informat.*, Jul. 2008, pp. 889–892, doi: 10.1109/INDIN.2008.4618227.

[8] J. P. Merlet, *Parallel Robots*, vol. 128. Dordrecht, The Netherlands: Springer, 2006.

[9] N. Leroy, A. M. Kokosy, and W. Perruquetti, "Dynamic modeling of a parallel robot. Application to a surgical simulator," in *Proc. IEEE Int. Conf. Robot. Automat.*, vol. 3, Sep. 2003, pp. 4330–4335, doi: 10.1109/ROBOT.2003.1242270.

[10] Y. X. Su, B. Y. Duan, B. Peng, and R. D. Nan, "Singularity analysis of fine-tuning Stewart platform for large radio telescope using genetic algorithm," *Mechatronics*, vol. 13, no. 5, pp. 413–425, 2003, doi: 10.1016/S0957-4158(01)00051-4.

[11] G. Lebret, K. Liu, and F. L. Lewis, "Dynamic analysis and control of a Stewart platform manipulator," *J. Robotic Syst.*, vol. 10, no. 5, pp. 629–655, Jul. 1993, doi: 10.1002/rob.4620100506.

[12] Q. Wang, "Closed form direct kinematics of a class of Stewart platform," *IFAC Proc. Volumes*, vol. 35, no. 1, pp. 211–215, 2002.

[13] L.-W. Tsai, "Solving the inverse dynamics of a Stewart-Gough manipulator by the principle of virtual work," *J. Mech. Des.*, vol. 122, no. 1, pp. 3–9, Mar. 2000, doi: 10.1115/1.533540.

[14] B. Dasgupta and T. S. Mruthyunjaya, "Closed-form dynamic equations of the general Stewart platform through the Newton–Euler approach," *Mech. Mach. Theory*, vol. 33, no. 7, pp. 993–1012, 1998, doi: 10.1016/S0094-114X(97)00087-6.

[15] H. Q. Wang, W. Bai, and P. Liu, "Finite-time adaptive fault-tolerant control for nonlinear systems with multiple faults," *IEEE/CAA J. Automatica Sinica*, vol. 6, no. 6, pp. 1417–1427, Nov. 2019, doi: 10.1109/JAS.2019.1911765.

[16] M. Van, M. Mavrovouniotis, and S. S. Ge, "An adaptive backstepping nonsingular fast terminal sliding mode control for robust fault tolerant control of robot manipulators," *IEEE Trans. Syst., Man, Cybern., Syst.*, vol. 49, no. 7, pp. 1448–1458, Jul. 2018, doi: 10.1109/TSMC.2017.2782246.

[17] Q. Shen, B. Jiang, and V. Cocquempot, "Adaptive fuzzy observer-based active fault-tolerant dynamic surface control for a class of nonlinear systems with actuator faults," *IEEE Trans. Fuzzy Syst.*, vol. 22, no. 2, pp. 338–349, Apr. 2014, doi: 10.1109/TFUZZ.2013.2254493.

[18] B. Li, K. Qin, B. Xiao, and Y. Yang, "Finite-time extended state observer based fault tolerant output feedback control for attitude stabilization," *ISA Trans.*, vol. 91, pp. 11–20, Aug. 2019, doi: 10.1016/j.isatra.2019.01.039.

[19] C. Edwards, S. K. Spurgeon, and R. J. Patton, "Sliding mode observers for fault detection and isolation," *Automatica*, vol. 36, no. 4, pp. 541–553, 2000, doi: 10.1016/S0005-1098(99)00177-6.

[20] K. K. Hassan and P. Laurent, "High-gain observers in nonlinear feedback control," *Int. J. Robust Nonlinear Control*, vol. 24, no. 6, pp. 993–1015, Jul. 2014, doi: 10.1002/rnc.3051.

[21] J. H. Ahrens and H. K. Khalil, "High-gain observers in the presence of measurement noise: A switched-gain approach," *Automatica*, vol. 45, no. 4, pp. 936–943, Apr. 2009, doi: 10.1016/j.automatica.2008.11.012.

[22] L. B. Freidovich and H. K. Khalil, "Performance recovery of feedback-linearization-based designs," *IEEE Trans. Autom. Control*, vol. 53, no. 10, pp. 2324–2334, Nov. 2008, doi: 10.1109/TAC.2008.2006821.

[23] M. Ran, Q. Wang, C. Dong, and L. Xie, "Active disturbance rejection control for uncertain time-delay nonlinear systems," *Automatica*, vol. 112, no. 11, pp. 5830–5836, 2020, doi: 10.1016/j.automatica.2019.108692.

[24] M. Ran, J. Li, and L. Xie, "A new extended state observer for uncertain nonlinear systems," *Automatica*, vol. 131, Sep. 2021, Art. no. 109772, doi: 10.1016/j.automatica.2021.109772.

[25] M.-S. Chen, Y.-R. Hwang, and M. Tomizuka, "A state-dependent boundary layer design for sliding mode control," *IEEE Trans. Autom. Control*, vol. 47, no. 10, pp. 1677–1681, Oct. 2002, doi: 10.1109/TAC.2002.803534.

[26] H.-M. Chen, J.-C. Renn, and J.-P. Su, "Sliding mode control with varying boundary layers for an electro-hydraulic position servo system," *Int. J. Adv. Manuf. Technol.*, vol. 26, nos. 1–2, pp. 117–123, Jul. 2005, doi: 10.1007/s00170-004-2145-0.

[27] V. Utkin, "Discussion aspects of high-order sliding mode control," *IEEE Trans. Autom. Control*, vol. 61, no. 3, pp. 829–833, Mar. 2016, doi: 10.1109/TAC.2015.2450571.

[28] J. J. Rath, M. Defoort, H. R. Karimi, and K. C. Veluvolu, "Output feedback active suspension control with higher order terminal sliding mode," *IEEE Trans. Ind. Electron.*, vol. 64, no. 2, pp. 1392–1403, Feb. 2017.

[29] W. Gao and J. C. Hung, "Variable structure control of nonlinear systems: A new approach," *IEEE Trans. Ind. Electron.*, vol. 40, no. 1, pp. 45–55, Feb. 1993, doi: 10.1109/41.184820.
[30] T. Wang, M. Zhao, Y. Li, and K. Liu, "Double-power reaching law sliding mode control for spacecraft decline based on radial basis function networks," in *Proc. 29th Chin. Control Decis. Conf. (CCDC)*, May 2017, pp. 5396–5401, doi: 10.1109/CCDC.2017.7979456.
[31] M. Tao, Q. Chen, X. He, and M. Sun, "Adaptive fixed-time fault-tolerant control for rigid spacecraft using a double power reaching law," *Int. J. Robust Nonlinear Control*, vol. 29, pp. 4022–4040, Apr. 2019, doi: 10.1002/rnc.4593.
[32] C. J. Fallaha, M. Saad, H. Y. Kanaan, and K. Al-Haddad, "Sliding-mode robot control with exponential reaching law," *IEEE Trans. Ind. Electron.*, vol. 58, no. 2, pp. 600–610, Feb. 2011, doi: 10.1109/TIE.2010.2045995.
[33] G.-Y. Yang and S.-Y. Chen, "Piecewise fast multi-power reaching law: Basis for sliding mode control algorithm," *Meas. Control*, vol. 53, nos. 9–10, pp. 1929–1942, Nov. 2020, doi: 10.1177/0020294020964246.
[34] B.-Z. Guo and Z.-L. Zhao, "On the convergence of an extended state observer for nonlinear systems with uncertainty," *Syst. Control Lett.*, vol. 60, pp. 420–430, Jun. 2011, doi: 10.1016/j.sysconle.2011.03.008.
[35] Y. Li and S. Tong, "Adaptive neural networks decentralized FTC design for nonstrict-feedback nonlinear interconnected large-scale systems against actuator faults," *IEEE Trans. Neural Netw. Learn. Syst.*, vol. 28, no. 11, pp. 2541–2554, Nov. 2017, doi: 10.1109/TNNLS.2016.2598580.

DUC-VINH LE received the B.S. degree in mechatronics engineering from the Da Nang University of Technology, Da Nang, Vietnam, in 2011. He is currently pursuing the master's degree with the Graduate School of Mechanical Engineering, University of Ulsan, Ulsan, South Korea. His current research interests include robust control and intelligent control.

CHEOLKEUN HA received the B.S. and M.S. degrees in aeronautical engineering from Seoul National University, in 1984 and 1986, respectively, and the Ph.D. degree from University of Washington (UW), in 1993. In 1993, he worked as a Postdoctoral Researcher at UW. Since 1993, he has been a Professor at University of Ulsan, South Korea. His research interests include motion control of mechanical dynamic systems, autonomous flight control of aerial vehicles, visible light positioning of a moving vehicle, and computer vision for industrial applications.